Letters

Unified Viewpoint of Soft Startup and Rate Limiter for SOGI-FLL

Wenshuai Shi, Jingrong Yu, and Ying Guo

***Abstract*—This letter demonstrates that the second-order generalized integrator-based frequency-locked loop (SOGI-FLL) with a soft startup/rate limiter essentially incorporates an adaptive feedforward relying on *a priori* information of transient input. When a fair parameter is tuned, the soft startup and the limiter give a similar performance. The shortcoming is that they have a deceleration blind zone, depending on the frequency constraints and SOGIs gain. If the allowed rate of change of frequency (RoCoF) is fixed, the fast response FLL can weaken this shortcoming. Specifically, if the RoCoF of low-inertia grids is considered, they could produce a severely biased estimation under the harmonics and dc offsets. The experimental results are given to validate the claims.**

***Index Terms*—Frequency-locked loop (FLL), rate limiter, soft startup, transient analysis.**

I. Introduction

TO ESTIMATE the frequency of single-phase or unbalanced grid voltages in real time, the second-order generalized integrator-based frequency-locked loop (SOGI-FLL, in Fig. 1) has enjoyed enormous popularity due to its concise structure [1], [2]. However, a drawback of SOGI-FLL is that its frequency response will suffer from a significant fluctuation under phase jump and voltage sag (see Fig. 2). In [3] and [4], Karimi Ghartemani *et al.* propose the famous soft startup strategy to overcome this problem by reducing the dynamic coupling between the phase and frequency. In [5] and [6], the frequency rate limiter is considered to restrict its frequency response directly.

The mentioned soft startup/limiter is started from different perspectives and obeys different parameter tunings. Meanwhile, they both have an efficient improvement. Based on this description, readers may have some confusion as follows.

1) Is it necessary to use them simultaneously?
2) How do analytically tune them for fewer efforts?
3) What are their shortcomings?

This letter will answer them from a unified viewpoint.

Manuscript received 8 March 2022; revised 17 April 2022; accepted 5 June 2022. Date of publication 10 June 2022; date of current version 26 July 2022. *(Corresponding authors: Jingrong Yu; Ying Guo.)*

The authors are with the School of Automation, Central South University, Changsha 410083, China (e-mail: scdyljsws@163.com; jingrong_yu@126.com; yingguo@csu.edu.cn).

Color versions of one or more figures in this article are available at https://doi.org/10.1109/TPEL.2022.3181335.

Digital Object Identifier 10.1109/TPEL.2022.3181335

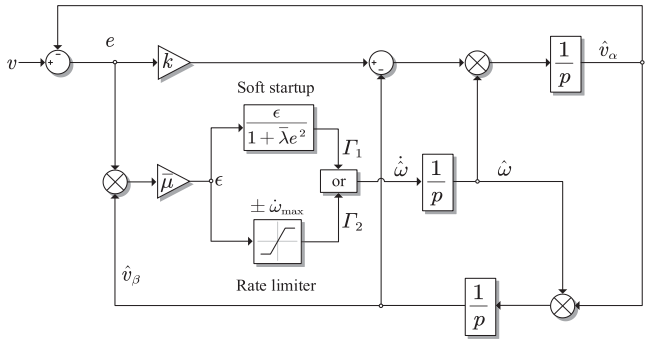

Fig. 1. Block diagram of SOGI-FLL with soft startup or frequency rate limiter, where the module "OR" denotes the independent element Γ_1 or Γ_2.

II. Unified Viewpoint

First, a clean input signal v is defined as

$$v \triangleq A\cos(\omega t+\varphi) \tag{1}$$

where "$\triangleq$" defines the left variable as the right expression; t is the current time; A, φ, and ω are the amplitude, initial phase, and angular frequency, respectively.

To identify the frequency ω, the SOGI-FLL is given by

$$\begin{cases} \hat{v}_\alpha = v\left[\frac{k\hat{\omega}p}{p^2+k\hat{\omega}p+\hat{\omega}^2}\right], \quad \hat{v}_\beta = \hat{v}_\alpha\left[\frac{\hat{\omega}}{p}\right] \\ \dot{\hat{\omega}} = \epsilon \triangleq \bar{\mu}\hat{v}_\beta(\underbrace{v-\hat{v}_\alpha}_{e}) \end{cases} \tag{2}$$

where $\hat{v}_\alpha$ and $\hat{v}_\beta$ are the estimated signals, $\hat{\omega}$ is the estimated frequency, and $\bar{\mu}$ is the gain of FLL.

Notations: The sign $o \triangleq i[\mathcal{F}(p)]$ defines the *time-domain relationship* between input $i(t)$ and output $o(t)$ by an operator $\mathcal{F}(p)$, and p denotes the derivative operator with t (i.e., $o=i[p] \Leftrightarrow o=\dot{i}$). In particular, when the operator $\mathcal{F}(p)$ is a linear time-invariant system, the operator p is equivalent to the Laplace operator s.

For the FLLs gain in (2), a standard design is given by

$$\bar{\mu} \triangleq -\frac{\mu}{\hat{v}_\alpha^2+\hat{v}_\beta^2}. \tag{3}$$

This design can assure fast frequency tracking under severe voltage sag due to the amplitude normalization gain $(\hat{v}_\alpha^2+\hat{v}_\beta^2)^{-1}$. In some classic works [7], [8], the frequency normalization gain $(1+c\hat{\omega}^2)^{-1}$ is also considered, where $c>0$

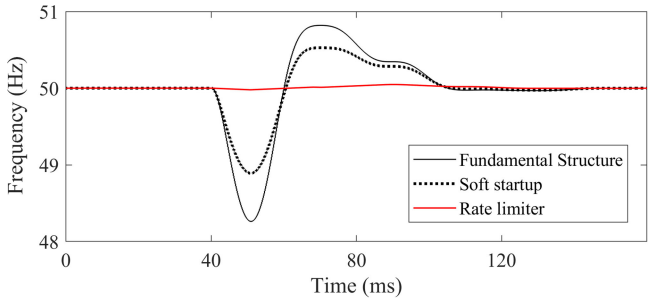

Fig. 2. Frequency response of SOGI-FLLs under 20% voltage sag, where $k = 1.414$, $\mu = 49\,384$, $\lambda = 100$, and $\dot{\omega}_{\max} = 8\pi$.

is a small constant. The following analysis will be given based on the standard design in (3), but the frequency normalization's effect will also be clarified.

A. Motivation

As shown in Fig. 2, the fundamental structure suffers from a significant fluctuation. The soft startup strategy is given by

$$\begin{cases} \dot{\hat{\omega}} = \mathbf{\Gamma}_1 \triangleq \frac{\epsilon}{1+\bar{\lambda}\epsilon^2} \\ \bar{\lambda} = \frac{\lambda}{\hat{v}_\alpha^2 + \hat{v}_\beta^2} \end{cases} \tag{4}$$

to reduce the dynamic coupling between the phase and frequency. When the energy of normalization error is enormous, the FLL gain will become small while maintaining the original performance when the energy is zero. Here, the energy is defined as the power of a voltage $e/\sqrt{\hat{v}_\alpha^2 + \hat{v}_\beta^2}$ passing through the unit resistance. In particular, the gain λ controls the size of energy aggregation and dissipation.

On the other hand, an intuitive rate limiter is given by

$$\dot{\hat{\omega}} = \mathbf{\Gamma}_2 \triangleq \begin{cases} \epsilon, \text{if } |\epsilon| \le \dot{\omega}_{\max} \\ \dot{\omega}_{\max}, \text{if } |\epsilon| > \dot{\omega}_{\max} \end{cases} \tag{5}$$

to restrict the FLLs rate.

Usually, λ is tuned to be 50–100 for soft startup [3], [4] and the rate limiter satisfies the grid codes [9] (e.g., $\dot{\omega}_{\max} \le 2\pi \times 4\,\mathrm{Hz/s}$, for the low-inertia grids, where "s" is the second differs from operator *s*). A comparison is shown in Fig. 2. It shows that the limiter has a better improvement. However, it is doubtful whether this superiority is still established under the other grid conditions. This letter will give a unified viewpoint to answer this confusion. For expression conciseness, the soft startup or rate limiter is rewritten as $\dot{\hat{\omega}} = \mathbf{\Gamma}_{1,2}$.

B. Transient Input–Output Analysis

Unlike the definition in (1), the first step introduces the following definition with deterministic transient input:

$$v \triangleq A\cos(\underbrace{\omega t + \varphi}_{\phi}) + \delta \tag{6}$$

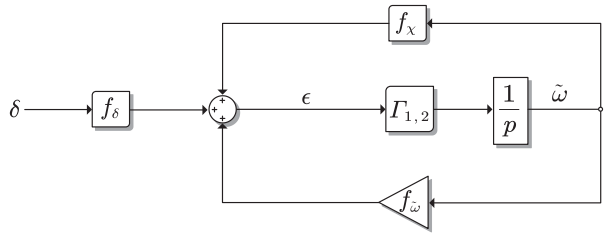

Fig. 3. Established input–output structure of SOGI-FLL with the soft startup or rate limiter.

and the transient input δ is expressed as

$$\delta = A\left(\lambda_1, \lambda_2, \lambda_3, \lambda_4\right) \begin{pmatrix} \delta_A(t) & 0 \\ \cos(\delta_\varphi(t)) - 1 & \sin(\delta_\varphi(t)) \\ \cos(\delta_\omega(t)t) - 1 & \sin(\delta_\omega(t)t) \\ \cos(\delta_r(t)t^2/2) - 1 & \sin(\delta_r(t)t^2/2) \end{pmatrix} \begin{pmatrix} \cos(\phi) \\ -\sin(\phi) \end{pmatrix} \tag{7}$$

where $\delta_x(t) = \delta_x u(t - t_1), \quad x \in \{A, \varphi, \omega, r\}$; $\delta_A \in [-1, 0]$, $|\delta_\varphi| \le \pi$, $|\delta_\omega| \le 10\pi$ are the allowed voltage/phase/frequency step range; $|\delta_r| \le 2\pi \times 4\,\mathrm{Hz/s}$ is the allowed rate of change of frequency (RoCoF) of low-inertia grids; $u(.)$ is the unit step function; t_1 is the initial time of the transient process; $\lambda_{1\text{–}4} = 1$, 0 denotes the disturbances exist or do not exist.

For the above assumptions, there are the following three points to be emphasized.

1) The input δ can be inversely obtained from a jumped signal
$$v = (A + \delta_A(t)) \times \cos\left\{(\omega + \delta_\omega(t))t + \varphi + \delta_\varphi(t) + \delta_r(t)t^2/2\right\}. \tag{8}$$
2) The assumption of frequency jump ($\le \pm 5$ Hz) is only for a comparative study of soft startup and rate limiter [1]–[3].
3) Since the soft startup and rate limiter aim to improve the transient response, the steady-state components, such as the harmonics and dc offsets, have not been considered for transient analysis. Nevertheless, this influence will be finally clarified.

Result 1: For an input signal satisfying (6) and the SOGI-FLL in Fig. 1, an input–output structure, as shown in Fig. 3, is given by

$$\begin{cases} \epsilon = f_{\tilde{\omega}}\tilde{\omega} + f_\delta + f_\chi \\ f_{\tilde{\omega}} = \mu_1 A \sin(\phi)(\hat{\omega} + \omega) \\ f_\delta = k\omega^2\mu_1\delta\left[\mathbf{\Lambda}(p)\right], \quad f_\chi = \mu_1\chi\left[\mathbf{\Lambda}(p)\right] \end{cases} \tag{9}$$

where the parameter $\tilde{\omega} \triangleq \hat{\omega} - \omega$ is the frequency estimation error, and the other parameters satisfy

$$\begin{cases} \mu_1 = \frac{\bar{\mu}\hat{v}_\beta}{k\hat{\omega}^2}, \quad \mathbf{\Lambda}(p) = \frac{p^2 + \hat{\omega}^2}{p^2 + k\omega p + \omega^2} \\ \chi = \tilde{\omega}((\hat{\omega} + \omega)(kv - \hat{v}_\beta) - k\dot{\hat{v}}_\beta). \end{cases}$$

Simplified Result 1: For a strict input–output structure, as shown in Fig. 3, a simplified version is shown in Fig. 4. Here, the corresponding estimation error is written as $\tilde{\omega}_\sim$ to prevent confusion with the error $\tilde{\omega}$ in Fig. 3.

The proof of the above results is given in Appendix. As shown in Fig. 3, the filtered transient input f_δ will be a null value for

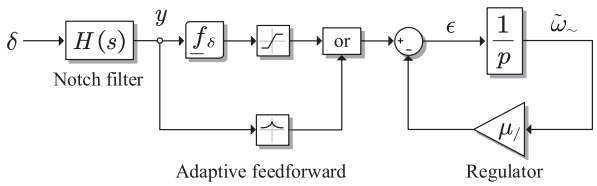

Fig. 4. Simplified version of the input–output structure, where $f_\delta \approx \underline{f}_\delta = -\mu \sin(\phi) y A^{-1}$, and $\mu_/ = \mu(k\omega)^{-1}$.

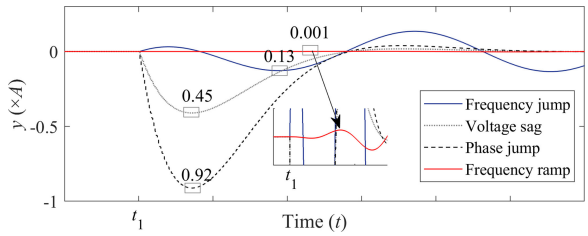

Fig. 5. Filtered transient input y under $+180^\circ$ phase-angle jump, 90% voltage sag, +5 Hz frequency jump, and +4 Hz/s ramp, where $k = 1.414$ for SOGI.

zero transient input δ. At this time, the frequency estimation error $\tilde{\omega}$ is also regulated to zero. When the parameters jump happens, δ will not be zero and will be dependent on f_δ. We can find that the approximated $\underline{f}_\delta$ is a notch-filtered signal y with a modulated signal, as shown in Fig. 4. Then, y is directly depicted in Fig. 5 to avoid too many mathematical components. For instance, parameters $\lambda_1 = 1$ and $\lambda_{2\text{–}4} = 0$ give the voltage sag. Fig. 5 can demonstrate the *a priori* information of transient input. The maximum y under phase jump/voltage sag is larger than the frequency jump for significant jump levels and far larger than the frequency ramp.

C. Unified Claims

By Figs. 3–5, the following claims are given.

1) *Adaptive feedforward:* $\Gamma_{1,\,2}$ makes the SOGI-FLL adaptive to the transient input f_δ and two frequency feedback paths $f_{\tilde{\omega}}, f_\chi$. When a considerable transient input is produced, $\Gamma_{1,\,2}$ can quickly adjust its gain regardless of the feedback, as shown in Fig. 4. This mechanism essentially utilizes the *a priori* information of transient input to assure effectiveness. Thus, it incorporates an adaptive feedforward to decouple the considerable transient input y for the frequency regulator if we consider the structure, as shown in Fig. 4, as a fundamental control problem.

Note that the control problem is described as follows: how to achieve good regulation performance for a deterministic transient input y and an integrator-based regulator? Naturally, if some features of the input y (i.e., *a priori* information) are known, we can control the input in advance without changing the regulator. This idea does not influence formal response speed if the control action is appropriately tuned.

Moreover, the transient performance of the feedforward controller relating to the parameters $\dot{\omega}_{\max}$, λ, and k can be concluded as follows.

a) Increasing the gains λ or reducing the rate $\dot{\omega}_{\max}$ can strengthen the feedforward action, yet the performance limit is dependent on δ_ω and δ_r.

b) Reducing the gain k can strengthen the feedforward action due to narrow notch ability but deteriorate the system's small disturbances response.

2) *Fair parameters tuning:* Since this adaptive feedforward uses the *a priori* information, a critical motivation is to determine whether there is a phase jump/voltage sag. Note that the maximum term under frequency jump is now a known value. Thus, the following fair parameters tuning is given to assure the soft startup, and the rate limiter does not affect the frequency tracking speed:

$$\begin{cases} \boldsymbol{\Gamma}_1 : \lambda \frac{y_F^2}{A^2} \ll 1 \Rightarrow \lambda \ll \frac{A^2}{y_F^2} \\ \boldsymbol{\Gamma}_2 : \dot{\omega}_{\max} \le \left| \underline{f}_\delta \right| \approx \mu \left| \sin(\phi) \right| \frac{y_F}{A} \le \mu \frac{y_F}{A}. \end{cases} \tag{10}$$

In (10), the term $y_F \triangleq \max_{t>t_1,\text{frequency}-\text{jump}} |y|$ is the maximum absolute value of y after the frequency jump ($>t_1$), which is determined by k and δ_ω. For instance, for $y_F = 0.13\,A$, it infers that $\lambda \ll 59, \dot{\omega}_{\max} \le 6400$ for $k = 1.4$, and $\mu = 49\,384$.

This tuning will validate the unified claim of soft startup and rate limiter from a comparative viewpoint by the step tests.

Furthermore, the frequency ramp case is focused on a realistic grid condition due to system inertia. The term y_F in (10) will depend on $|\delta_r|$, which satisfies $|\delta_r(t)|t^2/2 \ll \delta_\omega(t)t$, $\forall t \in (t_1, t_1 + \Delta t)$ over a tracking interval Δt (e.g., 0.02 s), as reflected in Fig. 5. Thus, the tuning of soft startup for low-inertia grids requires redefining y_F as the term $y_F \triangleq \max_{t>t_1,\text{frequency}-\text{ramp}} |y|$. Note that the rate limiter can be directly tuned since the RoCoF constraint is known.

3) *Deceleration blind zone:* $\Gamma_{1,\,2}$ exists a deceleration blind zone because $\max_{t>t_1} |y|$ under frequency jump is approximately seven times under severe phase jump and three times under severe voltage sag, according to Fig. 5. In other words, the deceleration blind zone could be the phase jump $<25^\circ$ and voltage sag <0.3 p.u. for $k = 1.414$ and ± 5 Hz jump. When the frequency ramp ± 4 Hz/s is considered rather than the jump, the blind zone will become very small since y_F has been reduced to 0.001 A. At this moment, the ineffective soft startup or rate limiter only happens for phase jump $<0.2^\circ$ and voltage sag <0.002 p.u.

If the allowed RoCoF $\dot{\omega}_{\max}$ is fixed, the blind zone will be amplified due to the slacked input $y_F = A\dot{\omega}_{\max}\mu^{-1}$ for a slow response FLL (i.e., low gain μ) required for high-accuracy measurement. In other words, the soft startup/limiter is more effective for a fast response FLL. A low-pass filter can improve the measurement accuracy, which relaxes the limitation of low gains.

4) *Frequency normalization:* As shown in the strict structure of Fig. 3, the input path f_δ and two feedback paths $f_{\tilde{\omega}}, f_\chi$ all include the gain $\bar{\mu}$. If the frequency normalization gain $(1 + c\hat{\omega}^2)^{-1}$ is incorporated, the loop couplings can be weakened for a significant frequency deviation due to reduced gain action. This logic helps us to understand why frequency normalization in [7] and [8] facilitates a smoother response under significant disturbances or even has a global convergence. However, the soft startup or rate limiter highly reduces the frequency fluctuations for the power grids (50/60 Hz) due to the utilization of the

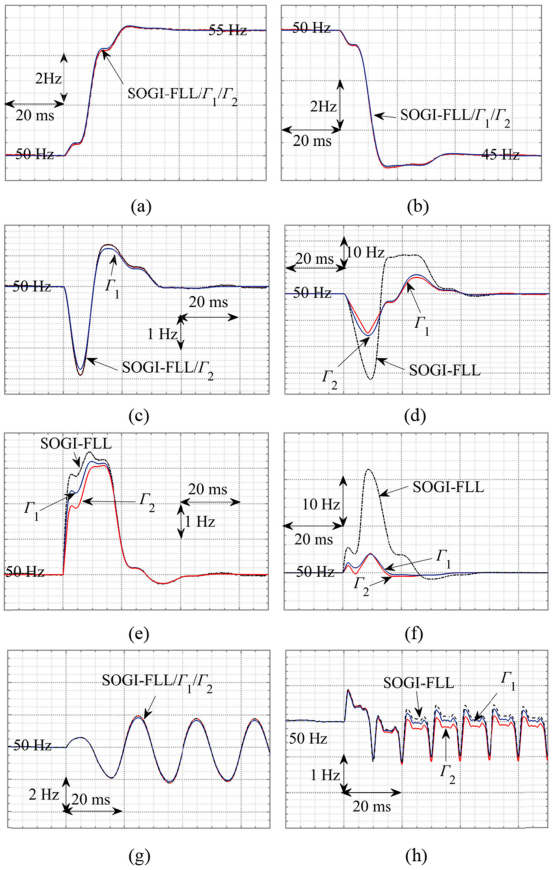

Fig. 6. Frequency response of SOGI-FLLs under case 1. (a) +5 Hz. (b) −5 Hz. (c) 30%. (d) 80%. (e) +20°. (f) +90°. (g) 5% dc offsets. (h) 5% 3th, 6% 5th, 5% 7th, 1.5% 9th, 3.5% 11th harmonics.

a priori frequency constraints. Thus, the improvement of frequency normalization could be minimal when the soft startup or rate limiter is incorporated.

5) *Harmonics and dc offsets pollution:* Although the soft startup has been tested to show no obvious influence on the steady-state performance for noise pollution [3], the case of harmonics and dc offsets pollution will be shown to have an inconsistent phenomenon.

This phenomenon is divided into the following twofold.

a) No influence when the input y under frequency jump/ramp is larger than the input y for harmonics and dc offsets.

b) Poorly biased estimation when the mentioned relationship is converse. For an intuitive understanding, the readers can jump into Fig. 7(c) and (d) for quick recognition.

Now, the reason behind this phenomenon will be clarified. Note that the input–output structure is still effective for harmonics and dc offsets since the derivation process does not use the input expression of δ. Hence, the filtered input y will be a steady-state signal for dc offsets or harmonics. For instance, given 15% dc offsets, y is still 0.15 A since the notch filter does not attenuate the dc offsets. Interestingly, when the mentioned claim in adaptive feedforward is considered, the regulator will cause an erroneous transient improvement under ±5 Hz frequency jump constraints (i.e., $y = 0.13\,A$).

In particular, if the soft startup and rate limiter are tuned based on the RoCoF constraint of low-inertia grids (i.e., $y_F = 0.004\,A$),

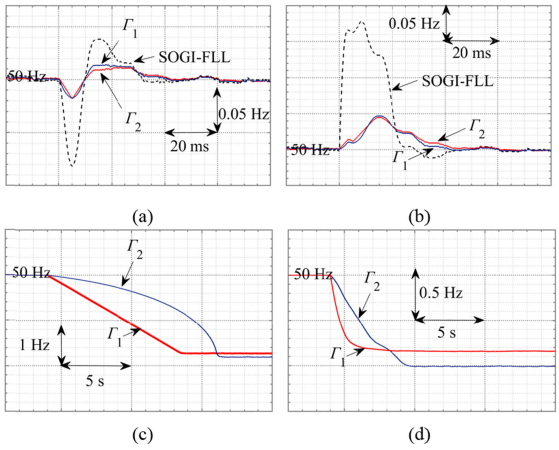

Fig. 7. Frequency response of SOGI-FLLs under case 2. (a) 1% voltage sag. (b) +1° phase jump. (c) 5% dc offsets. (d) 5% 3th, 6% 5th, 5% 7th, 1.5% 9th, 3.5% 11th harmonics, where the removed waves of SOGI-FLL in (c), (d) are the same in Fig. 6(g) and (h).

the estimated frequency will have a poor steady-state bias. This shortcoming is because a "stronger" soft startup or rate limiter is more sensitive to dc offsets and harmonics.

Technically speaking, the soft startup and rate limiter destroy the linearity of harmonics and dc offsets, making the regulator's input not satisfy the superposition principle. Thus, the frequency regulation error $\tilde{\omega}_\sim$ will not be a simple periodic oscillation, a common phenomenon for standard SOGI-FLL, as shown in Fig. 6(g) and (h). At this time, one must carefully solve the dc offsets and harmonics pollutions rather than simply filtering the estimated frequency.

In a simple word, the dc offsets/harmonics could make the soft startup and limiter fail to identify whether the frequency happens a change, which produces a severely biased estimation.

III. Experimental Validation

In this part, the fundamental SOGI-FLL, SOGI-FLL with Γ_1 and Γ_2 will be validated by experimental tests. The sampling frequency is $f_s = 12.8$ kHz, and the nominal frequency is $f_N = 50$ Hz. The discretization of SOGI uses the relatively accurate third-order integrator method without the algebraic loop. The voltage generated by a programmable ac source is converted to the digital signal by an external A/D sampling board involving hall sensors, 16-bit-ADS8556, and a signal conditioning circuit. DSP F28335 executes the C-codes of FLLs, and Code composer studio (CCS)-6.0 obtains the estimated frequency to drawing software for convenient comparison.

Table I lists the experimental test designs, and Table II lists the tuned parameters of SOGI-FLLs. Due to space restriction, the input waveform is not shown (initial phase $\varphi = -90°$).

From Fig. 6(a) and (b), they do not influence the frequency tracking speed even under a significant frequency jump, which is consistent with the claim in (10). Fig. 6(c) reflects the deceleration blind zone that makes these methods ineffective, while their frequency response is highly improved under large voltage sag, as shown in Fig. 6(d). Similarly, Fig. 6(e) and (f) obtains consistent conclusions. In conclusion, the inherent shortcomings of these methods are the deceleration blind zone. There are

TABLE I
TEST DESIGNS OF SOGI-FLLS

Designs	Cases	Grid conditions
Comparative tests using step disturbances[1]	1	Frequency jump, voltage sag, phase jump, DC-offsets or harmonics
RoCoF constraint of low-inertia grids[2]	2	Phase jump, voltage sag, DC-offsets, or harmonics
Different bandwidths	3	Voltage sag, phase jump under harmonics and DC-offsets

[1]The step disturbances are convenient to see the performance differences between the soft startup and rate limiter. This design is only for comparative study, as considered in [1]–[3].
[2]The RoCoF of future low-inertia grid frequency is required to satisfy $\leq \pm 4$ Hz/s in ([9], Table II), and the voltage sag is set to be $\leq 50\%$ for a mandatory or permissive low-voltage ride-through operation in ([11], Fig. 12).

TABLE II
PARAMETERS OF SOGI-FLLS

Cases	Tuned parameters[1]
1, 3[2] (y_F=0.13 A)	k=1.414, μ=49384, λ=5, $\omega_{\max}=2000\pi$
	k_S=1.414, μ_S=49384 and k_F=1.414/4, μ_F=49384/16, $\omega_{\max}=2000\pi$
2 (y_F=0.001 A)	k=1.414, μ=49384, $\lambda=3\times10^5$, $\omega_{\max}=8\pi$

[1]The parameters k, μ obey the optimum tuning of SOGI-FLL in [[1], eq. (28)]; the soft startup gain λ and rate limiter $\dot{\omega}_{\max}$ obey the given tuning in (10); the parameters subscripts "F, S" denote SOGI-FLL with fast response and slow response, respectively.
[2]The rate limiter $\dot{\omega}_{\max}=2000\pi$ is considered in case 3 for preventing the poorly biased estimation since only the fundamental SOGI-FLL is considered.

no apparent differences between them in terms of frequency response.

Fig. 6(g) and (h) shows no apparent difference between the compared methods under dc offsets and harmonics pollution. The considered frequency jump constraint is very slacked since the term y_F is not far smaller than the proportion of dc offsets and harmonics. Thereby, the biased estimation is not apparent.

Fig. 7(a) and (b) compares the frequency response of SOGI-FLLs considering the RoCoF constraint of low-inertia grids. It is found that there is still a similar performance between the soft startup and rate limiter. The transient improvement is also effective under a minimal phase jump and voltage sag.

Moreover, Fig. 7(c) and (d) gives the uncommon phenomenon that the frequency estimation is slowly convergent to a biased value rather than polluted with the periodic oscillation around 50 Hz, which are shown in Fig. 6(g) and (h). This phenomenon is attributed to the erroneous identification of transient disturbances, pointed out in Section II-C.

In summary, the rate limiter or soft startup following the RoCoF constraint of low-inertia grids can highly improve the frequency response of SOGI-FLL. However, a poor biased estimation is produced under dc offsets and harmonics. There is still an unavoidable compromise for SOGI-FLL between the transient fluctuations and the estimation accuracy even when the tracking speed is maintained.

Fig. 8 compares the SOGI-FLLs with different bandwidths under distorted grid conditions. Here, the 1.5% dc offsets, 2% 3th, 3% 5th, 2% 7th, 0.5% 9th, and 1% 11th harmonics are

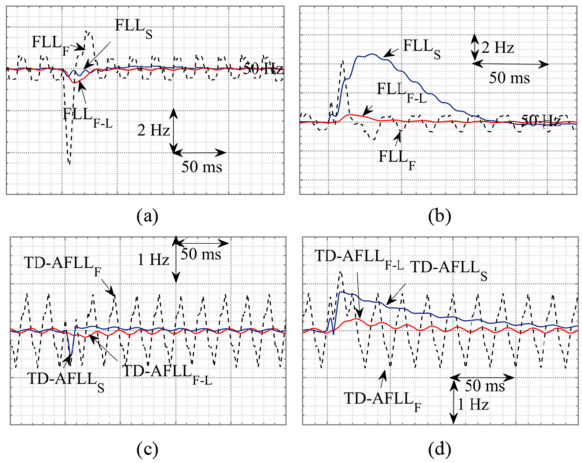

Fig. 8. Frequency response of FLLs under case 3. (a) 50% voltage sag. (b) +90° phase jump. (c) 50% voltage sag. (d) +90° phase jump, where (a, b) for SOGI-FLL and (c, d) for TD-AFLL.

considered. The additional low-pass filter has a time constant of 0.02 s for a fair comparison with the slow response FLL. In Fig. 8, the transient improvement of the limiter is strengthened when the fast response FLL (FLL_F) is used, which denotes that the corresponding deceleration blind zone is reduced. In particular, when the low-pass filter ($\text{FLL}_{F\text{-}L}$) is added for higher measurement accuracy, the frequency response can be further improved.

The transfer delay-based adaptive frequency-locked loop (TD-AFLL) ([12], (14)) is also used to support the generality of the proposed viewpoint. The same conclusion can be obtained for TD-AFLL, as shown in Fig. 8, although the letter does not analyze the input–output structure of TD-AFLL. Here, TD-AFLLs gain is $\dot{\hat{\sigma}}=-\mu(v^2+v^2_{k-N/4})^{-1}e$, $|\dot{\hat{\sigma}}|\leq 5\times10^{-4}$ with $\mu=3200$ for TD-AFLL_F and $\mu=13$ for TD-AFLL_S.

It should be noted that this idea (i.e., fast response FLL with additional low-pass filter) essentially relaxes the frequency response limitation of rate limiter/soft startup in achieving a high-accuracy measurement objective. Although this idea increases the implementation complexity, its improvement is noticeable.

Besides, the unified viewpoint is also suitable for the other FLLs, such as TD-AFLL, which was validated by tests.

IV. CONCLUSION

This work unified the SOGI-FLL with a soft startup/rate limiter by transforming this complex system into a feedforward control problem. Some of the following confusions were answered.

1) It is unnecessary to apply them concurrently.
2) Proper tuning was given in (10) to avoid the trial-and-error method. This tuning showed no apparent performance difference between them.
3) Their inherent shortcoming was the deceleration blind zone, depending on the frequency constraints and the SOGIs gain.

The fast response FLL can weaken this shortcoming if the allowed RoCoF is fixed. Besides, the poorly biased estimation

was produced under dc offsets and harmonics if the RoCoF of low-inertia grids is required.

APPENDIX

Proof of results 1: For (2), there is no direct relationship between ϵ and $\dot{\hat{\omega}}$. Thus, rewriting ϵ as

$$\begin{aligned}\epsilon &= \overline{\mu}\hat{v}_\beta(v-\hat{v}_\alpha) = \overline{\mu}\hat{v}_\beta v\left[\frac{p^2+\hat{\omega}^2}{p^2+k\hat{\omega}p+\hat{\omega}^2}\right]\\ &= \overline{\mu}\hat{v}_\beta v\left[\frac{k\hat{\omega}^2}{p^2+k\hat{\omega}p+\hat{\omega}^2}\frac{p^2+\hat{\omega}^2}{k\hat{\omega}^2}\right]\\ &= \overline{\mu}\hat{v}_\beta\times\left(\hat{v}_\beta\left[\frac{p^2+\hat{\omega}^2}{k\hat{\omega}^2}\right]\right)\\ &= \frac{\overline{\mu}}{k\hat{\omega}^2}\hat{v}_\beta\times(\hat{v}_\beta\left[p^2+\hat{\omega}^2\right]).\end{aligned} \tag{A.1}$$

Note that $\hat{v}_\beta$ has

$$\hat{v}_\beta = v_\beta + \underbrace{\tilde{v}_\beta}_{\hat{v}_\beta - v_\beta} = A\sin(\phi) + \underbrace{\delta\left[\frac{k\omega^2}{p^2+k\omega p+\omega^2}\right]}_{\delta_f} + \tilde{v}_\beta \tag{A.2}$$

where the reference signal $v_\beta = v[k\omega^2(p^2+k\omega p+\omega^2)^{-1}]$.

By (A.1) and (A.2), a direct relationship related to the frequency estimation error $\tilde{\omega} \triangleq \hat{\omega}-\omega$ is given by

$$\begin{aligned}\epsilon = &\frac{\overline{\mu}}{k\hat{\omega}^2}\hat{v}_\beta\\ &\times\left\{A\sin(\phi)(\hat{\omega}+\omega)\tilde{\omega}+\delta_f\left[p^2+\hat{\omega}^2\right]+\tilde{v}_\beta\left[p^2+\hat{\omega}^2\right]\right\}.\end{aligned} \tag{A.3}$$

At the same time, the signal estimation error is related to

$$\begin{aligned}&k\hat{\omega}^2 v - k\omega^2 v = \ddot{\tilde{v}}_\beta + k\hat{\omega}\dot{\hat{v}}_\beta - k\omega\dot{v}_\beta + \hat{\omega}^2\hat{v}_\beta - \omega^2 v_\beta\\ &\Leftrightarrow \underbrace{\tilde{\omega}(\hat{\omega}+\omega)(kv-\hat{v}_\beta) - k\tilde{\omega}\dot{\hat{v}}_\beta}_{\chi} = \ddot{\tilde{v}}_\beta + k\omega\dot{\tilde{v}}_\beta + \omega^2\tilde{v}_\beta\\ &\Leftrightarrow \tilde{v}_\beta = \chi\left[\frac{1}{p^2+k\omega p+\omega^2}\right].\end{aligned} \tag{A.4}$$

Result 1 is proved through (A.3) and (A.4). Then, expanding f_δ as

$$\begin{cases} f_\delta = \overline{\mu}\hat{v}_\beta\frac{\omega^2}{\hat{\omega}^2}\delta\left[\underbrace{\frac{p^2+\omega^2}{p^2+k\omega p+\omega^2}}_{H(p)=H(s)} + \mathbf{\Lambda}_1(p,\tilde{\omega})\right]\\ \mathbf{\Lambda}_1(p,\tilde{\omega}) = \frac{(\hat{\omega}+\omega)\tilde{\omega}}{p^2+k\omega p+\omega^2}.\end{cases} \tag{A.5}$$

Since we only focus on how the deterministic input affects the transient response, rigorous stability analysis is not pursued in this letter. Then, omit the dynamic coupling term (i.e., $\tilde{\omega}\approx 0$), and f_δ is simplified as

$$\begin{cases} f_\delta = \underline{f}_\delta + \mathcal{O}(\tilde{\omega}) \approx \underline{f}_\delta\\ \underline{f}_\delta = \overline{\mu}v\left[\frac{k\omega^2}{p^2+k\omega p+\omega^2}\right]\underbrace{\delta\left[H(p)\right]}_{y}\end{cases} \tag{A.6}$$

where $\mathcal{O}$ has $\lim_{\tilde{\omega}\to 0}|\mathcal{O}(\tilde{\omega})/\tilde{\omega}|$, which is a constant.

Note that the above approximation is reasonable from the averaging viewpoint (see [10] with the same processing).

As observed in Fig. 3, $\Gamma_{1,\,2}$ is related to the paths: $f_{\tilde{\omega}}, f_\delta, f_\chi$. To simplify these paths, omit the frequency coupled and time-periodic terms as

$$\begin{cases} f_{\tilde{\omega}} = -\underbrace{\frac{\mu}{k\hat{\omega}^2}}_{\approx k\omega^2}\underbrace{\frac{A\sin(\phi)\hat{v}_\beta}{\hat{v}_\alpha^2+\hat{v}_\beta^2}}_{\approx 1/2}\underbrace{(\hat{\omega}+\omega)}_{\approx 2\omega} \approx -\underbrace{\frac{\mu}{k\omega}}_{\mu_/}\\ f_\chi = \mu_1\chi\left[\mathbf{\Lambda}(p)\right] = \mu_1\mathcal{O}(\tilde{\omega})\left[\mathbf{\Lambda}(p)\right]\approx 0\\ \underline{f}_\delta \approx -\frac{\mu}{A}\sin(\phi)y.\end{cases} \tag{A.7}$$

Thus, the *simplified result* 1 is proved, where the soft startup uses a similar relationship from (A.1)

$$\begin{aligned}e = &\frac{1}{k\hat{\omega}^2}\\ &\times\left\{A\sin(\phi)(\hat{\omega}+\omega)\tilde{\omega}+\delta_f\left[p^2+\hat{\omega}^2\right]+\tilde{v}_\beta\left[p^2+\hat{\omega}^2\right]\right\}\\ &= \delta_f\left[p^2+\omega^2\right]+\mathcal{O}(\tilde{\omega})+\mathcal{O}(\tilde{v}_\beta)\approx y\\ &\Rightarrow \frac{1}{1+\bar{\lambda}e^2}\approx\frac{1}{1+\lambda y^2A^{-2}}.\end{aligned} \tag{A.8}$$

REFERENCES

[1] S. Golestan, J. M. Guerrero, F. Musavi, and J. C. Vasquez, "Single-phase frequency-locked loops: A comprehensive review," *IEEE Trans. Power Electron.*, vol. 34, no. 12, pp. 11791–11812, Dec. 2019.

[2] J. Matas, H. Martín, J. de la Hoz, A. Abusorrah, Y. A. Al-Turki, and M. Al-Hindawi, "A family of gradient descent grid frequency estimators for the SOGI filter," *IEEE Trans. Power Electron.*, vol. 33, no. 7, pp. 5796–5810, Jul. 2018.

[3] M. Karimi Ghartemani, S. A. Khajehoddin, P. K. Jain, and A. Bakhshai, "Problems of startup and phase jumps in PLL systems," *IEEE Trans. Power Electron.*, vol. 27, no. 4, pp. 1830–1838, Apr. 2012.

[4] M. Karimi-Ghartemani, H. Karimi, S. A. Khajehoddin, and S. M. Hoseinizadeh, "Efficient modeling and systematic design of enhanced phase-locked loop structures," *IEEE Trans. Power Electron.*, vol. 37, no. 8, pp. 9061–9072, Aug. 2022.

[5] C. M. Hackl and M. Landerer, "Modified second-order generalized integrators with modified frequency locked loop for fast harmonics estimation of distorted single-phase signals," *IEEE Trans. Power Electron.*, vol. 35, no. 3, pp. 3298–3309, Mar. 2020.

[6] A. T. Nguyen and D.-C. Lee, "Advanced grid synchronization scheme based on dual eSOGI-FLL for grid-feeding converters," *IEEE Trans. Power Electron.*, vol. 37, no. 6, pp. 7218–7229, Jun. 2022.

[7] L. Hsu, R. Ortega, and G. Damm, "A globally convergent frequency estimator," *IEEE Trans. Autom. Control*, vol. 44, no. 4, pp. 698–713, Apr. 1999.

[8] G. Yin, L. Guo, and X. Li, "An amplitude adaptive notch filter for grid signal processing," *IEEE Trans. Power Electron.*, vol. 28, no. 6, pp. 2638–2641, Jun. 2013.

[9] J. Fang, H. Li, Y. Tang, and F. Blaabjerg, "On the inertia of future more-electronics power systems," *IEEE J. Emerg. Sel. Topics Power Electron.*, vol. 7, no. 4, pp. 2130–2146, Dec. 2019.

[10] F. Tedesco, A. Casavola, and G. Fedele, "Unbiased estimation of sinusoidal signal parameters via discrete-time frequency-locked-loop filters," *IEEE Trans. Autom. Control*, vol. 62, no. 3, pp. 1484–1490, Mar. 2017.

[11] S. Xu, Y. Xue, and L. Chang, "Review of power system support functions for inverter-based distributed energy resources—Standards, control algorithms, and trends," *IEEE Open J. Power Electron.*, vol. 2, pp. 88–105, Feb. 2021, doi: 10.1109/OJPEL.2021.3056627.

[12] Z. Dai, Z. Zhang, Y. Yang, F. Blaabjerg, Y. Huangfu, and J. Zhang, "A fixed-length transfer delay based adaptive frequency-locked loop for single-phase systems," *IEEE Trans. Power Electron.*, vol. 34, no. 5, pp. 4000–4004, May 2019.